

# Dynamical behaviour of photo-excited and voltage biased MQW structures with bistable electro-optical absorption

V A Kochelap<sup>†‡</sup>, L L Bonilla<sup>†</sup> and C A Velasco<sup>†§</sup>

<sup>†</sup> Universidad Carlos III de Madrid, Escuela Politécnica Superior,  
Av. Universidad 20, E-28911 Leganés, Spain

<sup>‡</sup> Institute of Semiconductor Physics, National Academy of Sciences, 252650 Kiev, Ukraine

Received 12 June 1998

**Abstract.** In this work we have studied the dynamics of switch-on and switch-off processes in biased MQW structures where every well shows optical bistability in a light intensity range ( $\mathcal{I}_l, \mathcal{I}_h$ ). We have analysed in detail MQW structures with negligible inter-well transport. We have found that the switch-on mechanism consists of a time sequence where every QW jumps into the high-absorption state. Therefore a step-like switching wave propagates through the structure. The switch-off process resembles a reverse wave propagating in the opposite direction and step-like processes in the plasma concentration decay. These effects can be used for conversion of an analogue optical signal to digital (optical and electrical) signal(s).

**Keywords:** Multiple quantum well heterostructures, electro-optical absorption, photoexcitation, bistability, multistability, dynamics

There are many quantum well heterostructures that show bistable electro-optical absorption: multiple quantum well heterostructures placed into the intrinsic region of a p-i-n diode connected to an electric circuit with a series resistor (self electro-optic effect devices (SEEDs)) [1–4]; similar structures with an open circuit [5, 6]; multiple quantum well structures placed between charged capacitor plates [7–9]; stacked asymmetric double and triple QWs [10], and others [11]. The bistable absorption arises due to the screening of the applied field by the photo-generated electrons and holes, which produces considerable changes in the optical spectra near the fundamental edge of absorption. These spectra become dependent on the concentration of the electron–hole plasma, i.e., on the intensity of the illumination. If the spectrum of the illuminating light is tuned into the region between exciton and interband absorption, the light absorption becomes bistable; i.e. for a given range of incident light intensities both low absorption (LA) state with low plasma concentration, and high absorption (HA) state with large plasma concentration can exist.

In these systems the dynamics of the switching processes between bistable states involves different physical processes: generation of excitons associated with the two-dimensional electron and hole sub-bands, fast exchange between exciton and electron–hole states, intra-well separation of electrons and holes, changes in their wavefunctions, and inter-well transport. Understanding these processes and their

manifestation in optics is important for both physics and its applications. In this work we study the dynamics of switch-on and -off processes in a voltage biased MQW structure without inter-well electron transfer, i.e., with an independent balance of the photo-excited plasma concentration for every QW. Electro-optical bistability in such structures was investigated in papers [7–9] under quasi-stationary conditions.

A model describing switching processes in optically bistable MQW structures should include a self-consistent calculation of electron–hole states in the wells (particularly sub-band energies,  $E_e, E_h$ , and wavefunctions,  $\Psi_e, \Psi_h$ ), the absorption factor  $A$ , and exciton and plasma concentrations ( $\mathcal{N}$ ). Two groups of characteristic timescales are important for the dynamics of switching. The first group comprises faster processes with characteristic quantum mechanical times  $\hbar/E_e, \hbar/E_p$ , and exchange times between exciton and electron–hole states,  $\tau_{ex}$ . The second group of time scales is related to the generation and recombination of the photo-generated carriers. These timescales can be estimated as  $\mathcal{N}_{ch}/AI$  and  $\tau_R$ , where  $\mathcal{N}_{ch}$  is a characteristic plasma concentration,  $I$  is a typical light intensity, and  $\tau_R$  is the recombination time. The timescales in the first group are considerably smaller than those in the second group. The dynamics of the system can be described by means of electron–hole states calculated at instantaneous plasma concentration  $\mathcal{N}(t)$ . This results in an exciton energy  $E_{ex}$ , which follows the position of the electron and hole sub-bands,

§ Author to whom correspondence should be addressed.

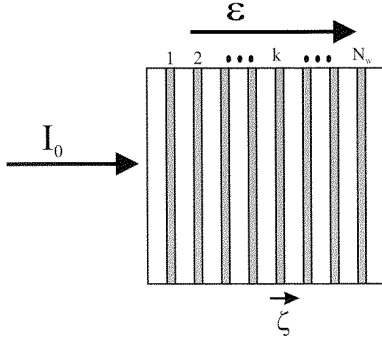


**Figure 1.** Scheme of a MQW heterostructure illuminated by incident light of intensity  $\mathcal{I}_0$  and biased by an electric field  $\mathcal{E}$ .

and an absorption factor adiabatically dependent on  $\mathcal{N}(t)$ . This approach is valid for light pulses with a duration of a few picoseconds or longer.

Let us consider a MQW structure biased by an electric field and illuminated from below, as illustrated in figure 1. The QWs have width  $2d$ , and are grown vertically along the  $\zeta$ -axis ( $\zeta$  is expressed in units of  $d$ ). Introducing the characteristic energy  $E_0 = \hbar^2/2md^2$ , we will measure sub-band energies and potential energies in these units, while the electric field is in units of  $\mathcal{E}_0 = E_0/ed$ . The dimensionless electron and hole concentrations ( $n$ ) are in units of  $\mathcal{N}_0 = \kappa E_0/e^2d$ ,  $\kappa$  being the dielectric permittivity. The  $k$ th QW ( $k = 1 \dots N_w$ ,  $N_w$  is the total number of QWs) can be described by its dimensionless electron and hole wavefunctions  $\psi_{e_k}$ ,  $\psi_{h_k}$ , sub-band electron and hole energies  $\epsilon_{e_k}$  and  $\epsilon_{h_k}$  (only the lowest sub-bands are supposed to be populated), and concentration of the photo-excited electron-hole plasma (supposedly quasi-neutral)  $n_k$ . We also assume that electrons and holes have equal effective masses for simplicity. According to the above discussion, the wavefunctions and energies of the  $k$ th QW can be found from the self-consistent Schrödinger-Poisson equation at a given plasma concentration  $n_k$ :

$$\frac{d^2\psi_k}{d\zeta^2} + (\epsilon_k + v_k - q\zeta)\psi = 0, \quad (1)$$

$$\psi_k(\pm 1) = 0, \quad \int_{-1}^1 |\psi_k(\zeta; n_k)|^2 d\zeta = 1,$$

where  $q$  is the dimensionless applied electric field, and the dimensionless electrostatic energy is

$$v_k(\zeta; n_k) = n_k \int_{-1}^1 d\zeta' \mathcal{K}(\zeta, \zeta') |\psi_k(\zeta'; n_k)|^2, \quad (2)$$

$$\mathcal{K}(\zeta, \zeta') \equiv \frac{1}{2}(|\zeta - \zeta'| - |\zeta + \zeta'|).$$

The electrostatic energy and the wavefunctions have the following symmetry properties:  $v_k(\zeta; n_k) = -v_k(-\zeta; n_k)$ , and  $\psi_{e_k}(\zeta; n_k) = \psi_{h_k}(-\zeta; n_k) = \psi_k(\zeta; n_k)$ . The eigenvalue  $\epsilon_k$  depends parametrically on  $n_k$ . We have found solutions of equation (1) by means of a variational method. The energy  $\epsilon_k$  as a function of  $n_k$  for a particular value of the electric field  $q$  is presented in figure 2(a). The parameters used in the calculations are given in table 1. The increase in the

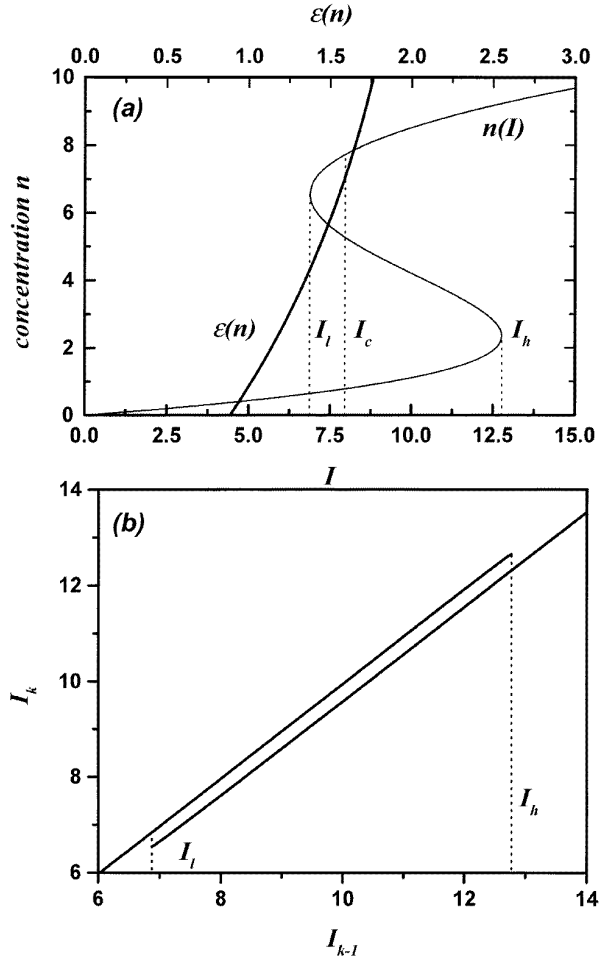


**Figure 2.** Steady state characteristics of individual QWs. (a) Shows the renormalized energy  $\epsilon$  (scale on top of the figure) as a function of the plasma concentration  $n$  (left axis), and bistable characteristic curve  $n(\mathcal{I})$ : plasma concentration as a function of the incident light intensity  $\mathcal{I}$  (left and bottom axis). (b) Shows the hysteresis in the transmitted light through a single QW.

**Table 1.** Numerical values used for calculation.

Parameter	Value
$E_0$ (meV)	5.6
$\mathcal{E}_0$ (kV cm <sup>-1</sup> )	5.6
$\mathcal{N}_0$ (cm <sup>-2</sup> )	$4.0 \times 10^{10}$
$\mathcal{I}_0/\hbar\omega$ (photons cm <sup>-2</sup> s <sup>-1</sup> )	$8.1 \times 10^{21}$

electron and hole energies with carrier concentration arises, obviously, from the screening of the applied field.

In the case of deep QWs and large exciton radius, the exciton energy  $E_{ex}$  follows the position of the electron and hole sub-bands. Assuming a Lorentz shape for the absorption factor as a function of the photon energy  $\hbar\omega$ , we can write:

$$A(n_k, q, \omega) = \frac{A_m \Lambda^2}{(\epsilon_k(n_k, q) - \Delta)^2 + \Lambda^2} \equiv A_m a(n_k, q, \omega), \quad (3)$$

where  $A_m$  is the maximum absorption factor,  $\Delta = (\hbar\omega + E_{ex} - E_g)/2E_0$  is the detuning of the photon energy, and  $\Lambda$  is the dimensionless bandwidth in units of  $2E_0$ .

We can describe the MQW structure in the case of

independent concentration balance for each QW by the following equations:

$$\frac{dn_k}{dt} = a(n_k, q, \omega)\mathcal{I}_{k-1} - n_k \equiv R(n_k, q, \omega, \mathcal{I}_{k-1}), \quad (4)$$

$$\mathcal{I}_k = (1 - A_m a(n_k, q, \omega))\mathcal{I}_{k-1}, \quad k = 1 \dots N_w. \quad (5)$$

Here we assume a linear recombination rate.  $t$  is measured in units of the recombination time  $\tau_R$ . For some particular parameters  $\omega$  and  $q$ , the stationary dependence  $n(\mathcal{I})$  is presented in figure 2(a).  $\mathcal{I}_{k-1}$  is the intensity illuminating the  $k$ th QW layer in units of  $\mathcal{I}_0 = N_0/\tau_R A_m$ . Thus,  $\mathcal{I}_0(t)$  is the incident light intensity. The instant relationship (5) between  $\mathcal{I}_k(t)$  and  $\mathcal{I}_{k-1}(t)$  requires the condition  $\frac{1}{\mathcal{I}_k(t)} \frac{d\mathcal{I}_k}{dt} \ll \frac{c(1-a)\tau_R}{2d}$ ,  $c$  being the velocity of light. This relation holds for pulses with a duration of a few picoseconds or longer. For a given  $\mathcal{I}_0(t)$ , and an initial concentration in every well  $n_k(0)$ , the system of equations (1)–(5) defines completely the dynamic problem for the MQW structure.

Let us consider the steady state condition. For this case, the equation

$$R(n_k, q, \omega, \mathcal{I}_{k-1}) = 0 \quad (6)$$

gives the possible solutions for the  $k$ th QW. It is easy to see that for the absorption factor of equation (3) there are *three branches* of uniform solutions  $n_k = n_k(\mathcal{I}, q)$  at some intervals of intensities  $\mathcal{I}$  and fields  $q$ : the low absorption branch (low concentration  $n_L(\mathcal{I})$ ), the high absorption branch (high concentration  $n_H(\mathcal{I})$ ) and the middle branch (which is unstable). In figure 2(b) we present these branches calculated for an individual QW for the particular parameter values of table 1. The bistable regime occurs in the interval  $\mathcal{I}_l < \mathcal{I} < \mathcal{I}_h$ . The light intensity transmitted through the  $k$ th QW layer shows hysteresis, as depicted in figure 2(b).

Using these solutions for an individual QW, we can easily construct possible steady states for the whole MQW structure. If the incident intensity  $\mathcal{I}_0$  is less than the value  $\mathcal{I}_l$ , the MQW structure is entirely in the LA state. If  $\mathcal{I}_l < \mathcal{I}_0 < \mathcal{I}_h$ , the whole structure can be in the LA state, or some of the QWs adjacent to the illuminated face can switch to the HA state. At  $\mathcal{I}_0 > \mathcal{I}_h$  the very first QW layers are certainly in the HA state, while the rest of wells can be in the LA state. In figure 3(a) the intensities  $\mathcal{I}_k$  as a function of the index  $k$  are presented for a 24-QW structure at  $\mathcal{I}_0 = 1.25 \times \mathcal{I}_h$ . The first seven QWs are always in the HA state and the intensity decreases quickly across this region of the structure. The QWs with  $k$  from 8 to 20 can be in both states. The QWs with  $k > 20$  are always in the LA state. This results in thirteen possible stationary states of the MQW structure. Three of these possible states are shown in the figure: (i) seven QWs in the HA state and the rest in the LA state, (ii) eight QWs in the HA state and the rest in the LA state, and (iii) the wells with  $k = 1 \dots 20$  are in the HA state, while the rest are in the LA state. The greater the intensity of the incident light,  $\mathcal{I}_0$ , the larger will be the number of QWs switched to the HA state. There is a critical value of the incident light intensity  $\mathcal{I}_0^*$ , dependent on the number of QWs of the structure, such that if  $\mathcal{I}_0 \geq \mathcal{I}_0^*$ , all the wells are switched to the HA state. Figure 3(b) depicts such a case for a 24-QW structure when  $\mathcal{I}_0 = 2\mathcal{I}_h$ . Thus, the bistability of the optical absorption in a single QW generally leads to *multistability* in the MQW structure. Which particular state

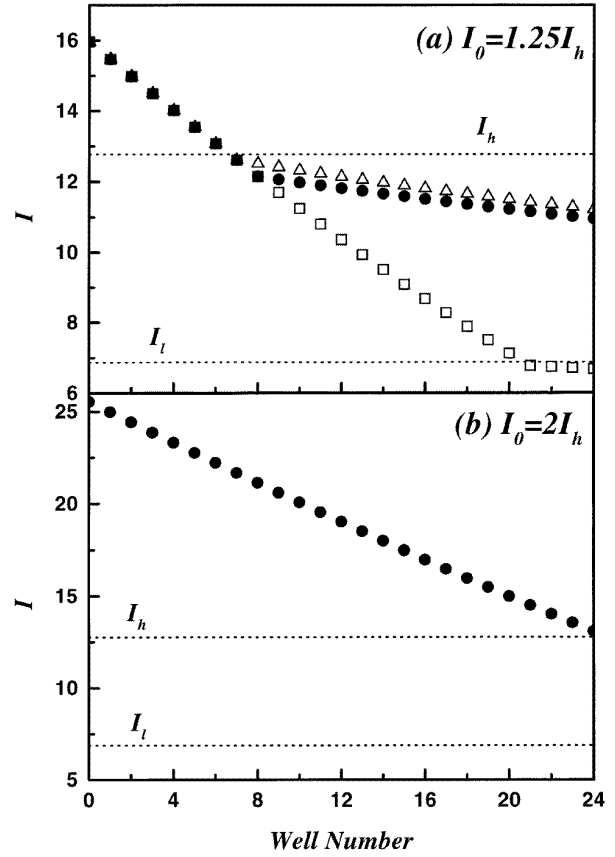


**Figure 3.** Distribution of intensities across the MQW structure. Positions of individual QWs are indicated. (a) Corresponds to incident light  $\mathcal{I}_0 = 1.25\mathcal{I}_h$ . Three of the possible 13 steady states described in the text are shown. Triangles correspond to case (i), circles correspond to case (ii) and squares correspond to case (iii). (b) Shows the steady state when  $\mathcal{I}_0 = 2\mathcal{I}_h$ . All the wells are in the HA state.

occurs depends on the prehistory, i.e., on the time dependence of the incident intensity,  $\mathcal{I}_0(t)$ , during the build-up of the stationary value<sup>†</sup>.

Let us go back to the dynamical problem and consider a time-dependent intensity of the incident light. We introduce the characteristic time scale of the build-up of the stationary light intensity value  $\tau_{in}$ , so that  $\mathcal{I} = \mathcal{I}(\frac{\tau_R}{\tau_{in}} t)$ . If

$$\beta \equiv \frac{\tau_R}{\tau_{in}} \ll 1, \quad (7)$$

we can perform a perturbative analysis. Let us rescale equation (4) introducing the new time variable:  $\bar{t} \equiv \beta t$ . Then we obtain that this equation can be rewritten as

$$\beta \frac{dn_k}{d\bar{t}} = a(n_k, q, \omega)\mathcal{I}_{k-1} - n_k \equiv R(n_k, q, \omega, \mathcal{I}_{k-1}). \quad (8)$$

Under condition (7), we can apply the boundary layer singular perturbation method to solve equation (8) (see, for example, [12]). According to this method, the solution

<sup>†</sup> If carriers may hop between QWs, the steady state distribution is, in principle, determined by this transfer. Let  $\tau_{int}$  be the characteristic time of the inter-well transport. A suppressed inter-well carrier transfer means  $\frac{\tau_R}{\tau_{int}} \ll 1$ . Thus, the results of our analysis are valid for  $\frac{1}{\bar{t}} \frac{d\bar{t}}{d\bar{t}} \gg \frac{\tau_R}{\tau_{int}}$ . If the latter inequality is not satisfied, the results are valid for times  $t \ll \frac{\tau_{int}}{\tau_R}$ .

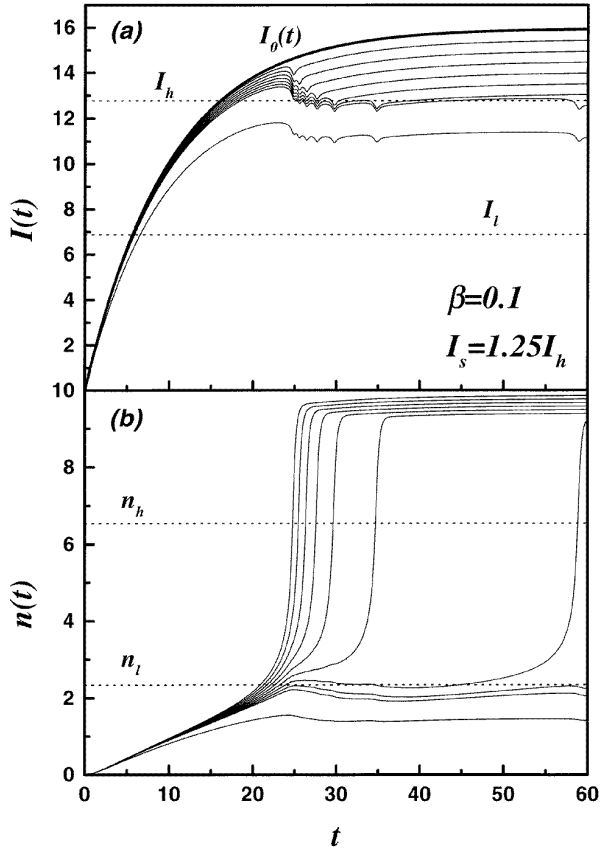


**Figure 4.** Dynamics of the MQW structure illuminated by the light intensity given by equation (12) at  $\mathcal{I}_s = 1.25 \times \mathcal{I}_h$  and  $\beta = 0.1$ . The critical intensity values  $\mathcal{I}_l$  and  $\mathcal{I}_h$  are shown. (a) Shows the incident intensity,  $\mathcal{I}_0(t)$ , and the intensities illuminating the first eight QWs and the transmitted intensity (the lower curve). (b) Shows the plasma concentrations for the same wells. The first seven QWs are switched to the HA state.

evolves smoothly over time intervals which last periods  $\bar{t} = O(1)$  separated by sharp transitions lasting times  $\bar{t} = O(\beta)$ . Outer solutions evolving on the long time scale  $\bar{t}$  can be found by treating the term multiplied by the small parameter  $\beta$  as a perturbation:

$$n_k(\bar{t}) = n_{k,0}(\bar{t}) + \beta n_{k,1}(\bar{t}) + O(\beta^2).$$

Here the leading term  $n_{k,0}(\bar{t})$  coincides with one of the two branches of the solutions of equation (6),  $n_L(\mathcal{I})$ ,  $n_H(\mathcal{I})$ , with  $\bar{t}$ -dependent  $\mathcal{I} = \mathcal{I}_{k-1}$ . The first correction to the outer solution is determined by

$$n_{k,1}(\bar{t}) = -\frac{1}{\left(\frac{\partial a(n_{k,0})}{\partial n_{k,0}} \mathcal{I}_{k-1}(\bar{t}) - 1\right)^2} \frac{d\mathcal{I}_{k-1}(\bar{t})}{d\bar{t}} a(n_{k,0}). \quad (9)$$

If the leading term lies on the low concentration branch,  $n_{k,0} = n_L[\mathcal{I}_{k-1}(\bar{t})]$ ,  $\mathcal{I}_{k-1} \leq \mathcal{I}_h$ , the first correction is small everywhere except in a vicinity of  $\bar{t} = \bar{t}_{k,h}$ , where  $\mathcal{I}_{k-1}(\bar{t}_{k,h}) = \mathcal{I}_h$  at  $(d\mathcal{I}/d\bar{t})_{\bar{t}_{k,h}} > 0$ . As  $\bar{t} \rightarrow \bar{t}_{k,h}$  the denominator term in equation (9) goes to zero. Similarly, when the leading term lies on the high concentration branch,  $n_{k,0} = n_H[\mathcal{I}_{k-1}(\bar{t})]$ ,  $\mathcal{I}_{k-1} \geq \mathcal{I}_l$ , the first correction is small everywhere, except in a vicinity of  $\bar{t} = \bar{t}_{k,l}$  with  $\mathcal{I}_{k-1}(\bar{t}_{k,l}) =$

$\mathcal{I}_l$ ,  $(d\mathcal{I}/d\bar{t})_{\bar{t}_{k,l}} < 0$ . For increasing  $\mathcal{I}_{k-1}(\bar{t})$  near  $\bar{t} = \bar{t}_{k,h}$ , and for decreasing  $\mathcal{I}_{k-1}(\bar{t})$  near  $\bar{t} = \bar{t}_{k,l}$ , the jumps between low concentration and high concentration solutions are described by inner solutions on the fast time scale  $t$ . To find the latter solutions we can keep  $\mathcal{I}_{k-1}(\bar{t}) = \mathcal{I}_h$  or  $\mathcal{I}_{k,h}(\bar{t}) = \mathcal{I}_l$  in equation (8) at  $t \approx \bar{t}_{k,h}$  and  $\bar{t} \approx \bar{t}_{k,l}$ , respectively. Then, the inner solutions are responsible for the process of fast switching between low and high concentration states. They have the form:

$$\int_{n_{h,l}}^n \frac{dn}{a(n)\mathcal{I}_{k-1,h,l} - n} = \pm \frac{\bar{t} - \bar{t}_{k,h,l}}{\beta}, \quad (10)$$

where  $n_h = n_H(\mathcal{I}_l)$ ,  $n_l = n_L(\mathcal{I}_h)$ . The sign ‘+’ corresponds to the inner solution determining switching from the low concentration to the high concentration branches at  $\mathcal{I}_{k-1} \approx \mathcal{I}_h$ , while the sign ‘-’ is for the inner solution joining high concentration to low concentration branches at  $\mathcal{I}_{k-1} \approx \mathcal{I}_l$ .

Now we obtain the evolution of the photo-excited plasma in the  $k$ th QW as follows. If the intensity of the light reaching this well,  $\mathcal{I}_{k-1}$ , increases from zero, the well is in the low absorption state with plasma concentration  $n = n_L[\mathcal{I}_{k-1}(\bar{t})]$  until  $\bar{t} < \bar{t}_{k,h}$ . In a vicinity of  $\bar{t}_{k,h}$  a fast switch-on process to the high absorption state with  $n = n_H[\mathcal{I}_{k-1}(\bar{t})]$  occurs according to equation (10). A further increase in the intensity leads to an increase in the plasma concentration and the absorption in accordance with the high absorption branch. If the intensity reaches a maximum and then decreases, the  $k$ th QW remains in this state up to time  $\bar{t} \approx \bar{t}_{k,l}$ , when a fast switch-off process (described by equation (10)) to the low absorption state occurs. As a result we have dynamic hysteresis for the  $k$ th QW. To be switched-on, the  $k$ th QW should accumulate plasma concentration up to  $n_h$ . The necessary time is estimated as  $\Delta\bar{t}_{\text{on}} \approx \beta(n_h - n_l)/n_h$ . The switch-off process occurs in a time  $\Delta\bar{t}_{\text{off}} \approx \beta$ . Important characteristics are the changes in the intensity  $\mathcal{I}_{k-1}$  during these fast stages. These changes are of the order of

$$\Delta\mathcal{I}_{k-1}^{\text{on}} \approx \Delta\bar{t}_{\text{on}} \left( \frac{d\mathcal{I}}{d\bar{t}} \right)_{\bar{t}_{k,h}} \approx \beta \frac{n_h - n_l}{n_l} \mathcal{I}_h,$$

$$\Delta\mathcal{I}_{k-1}^{\text{off}} \approx \Delta\bar{t}_{\text{off}} \left( \frac{d\mathcal{I}}{d\bar{t}} \right)_{\bar{t}_{k,l}} \approx \beta \mathcal{I}_l.$$

Let us suppose that  $\Delta\mathcal{I}_{k-1}^{\text{on}}$  and  $\Delta\mathcal{I}_{k-1}^{\text{off}}$  are small in comparison with the steady state attenuation in a single QW,  $a(n_k)\mathcal{I}_{l,h}$ . These conditions can be rewritten as

$$\beta \frac{n_h - n_l}{n_h} \ll a, \quad \beta \ll a. \quad (11)$$

If inequalities (11) are fulfilled, the times at which different QWs switch are well separated. Indeed, according to the above analysis, at the time  $\bar{t}_{1,h}$  when the very first QW switches to the HA state, the adjacent QWs follow adiabatically the intensity  $\mathcal{I}_1$ . At  $\bar{t}_2$ , the second QW switches-on, but the following QWs with  $k > 2$  still follow adiabatically the intensity  $\mathcal{I}_2$ , and so on. Thus we find that the MQW structure switches on sequentially as the intensity of light increases.

The reverse process—switch-off of the structure—occurs similarly. It starts when the intensity of light at the

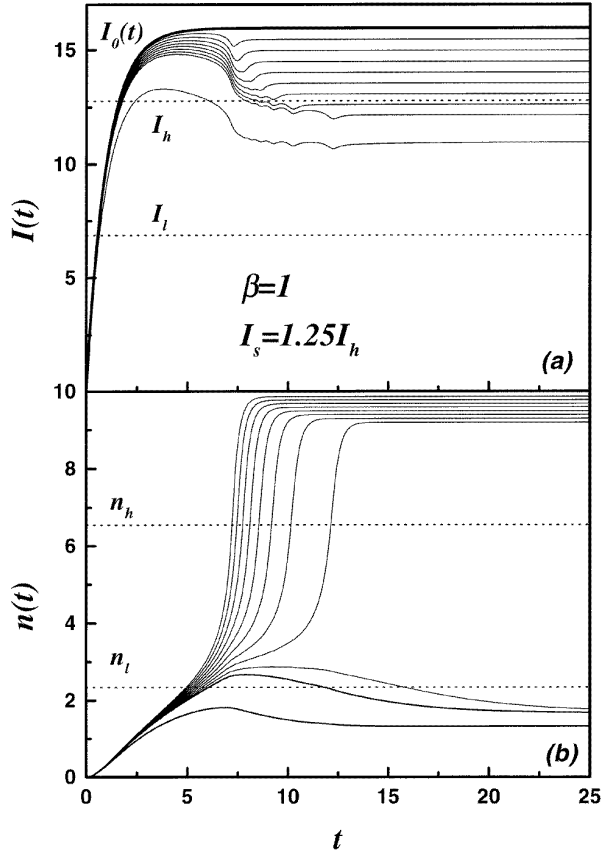


**Figure 5.** The same situation as in figure 4 with  $\beta = 1$ . Eight QWs are switched to the HA state at  $t \rightarrow \infty$ .

last QW in the HA state reaches the value  $I_l$ . Then a step-like ‘switch-off’ wave propagates towards the first QW.

The step-like propagation of a ‘switch-on wave’ through the structure was also found by direct numerical simulations. The results were obtained for a MQW structure with  $N_w = 24$  illuminated by an incident light of intensity

$$\mathcal{I}_0(t) = \mathcal{I}_s (1 - e^{-\beta t}). \quad (12)$$

In figure 4 we present numerical results for  $\mathcal{I}_s = 1.25 \times \mathcal{I}_h$  and  $\beta = 0.1$ . The intensities  $\mathcal{I}_{k-1}$  are shown as functions of  $t$  for  $k = 1 \dots 8$ . Nonmonotonic and sawtooth-like  $\mathcal{I}_{k-1}(t)$  ( $k = 2 \dots 8$ ) are due to the step-like switch-on of the QWs. In figure 4(b), the concentrations  $n_k(t)$  of the first nine QWs are shown. We clearly see that seven QWs switch in succession to the HA state at different times, while the other QWs remain in the LA state. As  $t \rightarrow \infty$  the input intensity saturates and the structure evolves to the steady state distribution presented in case (i) of figure 3(a).

The step-like character of the switching process obtained above in the limiting case (7) occurs also when  $\beta \sim 1$ . This is illustrated by the numerical simulations presented in figure 5 for a  $\mathcal{I}_0(t)$  given by equation (12) with  $\mathcal{I}_s = 1.25 \times \mathcal{I}_h$  and  $\beta = 1$ . As  $t \rightarrow \infty$  illumination with such an intensity results in a steady state distribution with eight QWs in the HA state (see case (ii) of figure 3(a)).

Increasing the light intensity leads to a larger number of QWs switching to the HA state. In figure 6 we present simulation results for an incident intensity given by

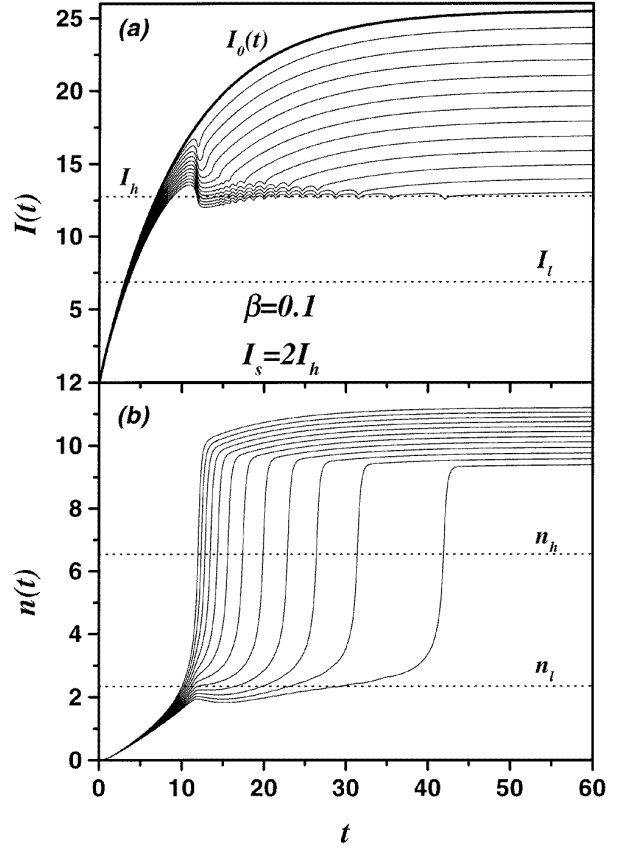


**Figure 6.** The same situation as in figures 4 and 5 with  $\mathcal{I}_s = 2 \times \mathcal{I}_h$  and  $\beta = 0.1$ . All the wells are switched to the HA state. Only wells with an odd index are shown.

equation (12) with  $\mathcal{I}_s = 2 \times \mathcal{I}_h$  and  $\beta = 0.1$ . From this figure we can see that the step-like switching process now involves all the QWs. For this intensity the final distribution corresponds to the steady state presented in figure 3(b). It is interesting to note that the output intensity is close to the value  $\mathcal{I}_h$ .

For a pulse illumination with a maximal intensity above  $\mathcal{I}_h$  both processes—switch-on and switch-off—take place. Using a Gaussian pulse:

$$\mathcal{I}_0(t) = \mathcal{I}_{\max} e^{-(\beta t)^2} \quad (13)$$

we found step-like switch-on and switch-off waves. In figure 7 we plot calculations of the transmitted intensity  $\mathcal{I}_{\text{out}}$ , as a function of the incident light intensity  $\mathcal{I}_0$ . The results were obtained for  $\mathcal{I}_{\max} = 1.25 \times \mathcal{I}_h$  and  $\beta = 0.1$ . Instead of a smooth hysteresis loop, we find one with a fine structure corresponding to the switch-on and switch-off processes.

It is interesting to recall that optical bistability with increasing absorption occurs also in bulk-like semiconductors. Different mechanisms underlying this type of bistability and different spatio-temporal patterns have been studied in [13–16]. For such systems, it has been found [17, 18] that if the diffusion of the photogenerated carriers is suppressed, switch-on and -off processes occur in a step-like propagating wave, which is quite similar to the above discussed results.

In conclusion, we have studied the dynamics of MQW structures under bistable electro-optical absorption. We

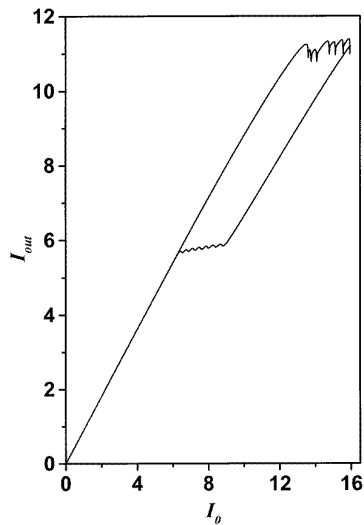


**Figure 7.** Output intensity versus input intensity for the pulse given by equation (13).

have formulated a model self-consistently describing the electron and hole wavefunctions and energies, and the processes of absorption, generation of the plasma and intra-well relaxation. The inter-well transfer has been supposed to be negligible. Under these conditions, steady state distributions of the intensity and plasma concentration are multistable. For time-dependent incident intensities we have found that switching processes between possible states of the structure occur as a result of sequential step-like switching of individual QWs. This leads to a characteristic behaviour of the transmitted intensity and input–output dependences. It is worth noticing that due to step-like switching we can use these MQW structures for the conversion of an analogue optical signal to digital (optical and electrical) signal(s).

### Acknowledgments

We are indebted to the Dirección General de Enseñanza Superior (Spanish Ministry of Education) for sabbatical support (VAK) and for financial support through grant PB94–0375. CAV acknowledges the support of the Fundación General de la Universidad Carlos III de Madrid.

### References

- [1] Miller D A B, Chemla D S, Damen T C, Wood T H, Burrus C A, Gossard A C and Wiegmann W 1985 *IEEE J. Quantum Electron.* **21** 1462
- [2] Schmitt–Rink S, Chemla D S and Miller D A B 1989 *Adv. Phys.* **38** 89–188
- [3] Lentine A L, Hinton H S, Miller D A B, Henry J E, Cunningham J E and Chirovski L M F 1989 *IEEE J. Quantum Electron.* **25** 1928
- [4] Miller D A B 1990 *Opt. Quantum Electron.* **22** S–61
- [5] Abe Y and Tokuda Y 1993 *Appl. Phys. Lett.* **63** 3259
- [6] Couturier J, Voisin P and Harmand J C 1994 *Appl. Phys. Lett.* **64** 742  
Couturier J, Voisin P and Harmand J C 1993 *J. Physique* **3–C5** 253  
Couturier J, Voisin P and Harmand J C 1995 *Semicond. Sci. Technol.* **10** 881
- [7] Merlin R 1989 Spectroscopy of semiconductor microstructures *NATO – Series B, Physics* **206** 347
- [8] Merlin R, Mestres N, McKiernan A, Oh J and Bhattacharya P K 1990 *Surf. Sci.* **228** 88–91
- [9] Merlin R and Kessler D A 1990 *Phys. Rev. B* **41** 9953
- [10] Trezza J A, Larson M C, Lord S M and Harris S J Jr 1993 *J. Appl. Phys.* **74** 1972  
Scandalo S and Tassone F 1992 *Phys. Status Solidi b* **173** 453
- [11] Bonilla L L, Kochelap V A, Sokolov V N and Velasco C A 1997 *Phys. Status Solidi b* **204** 559–62
- [12] Kevorkian J and Cole J D 1981 *Perturbation Methods in Applied Mathematics* (New York: Springer)
- [13] Kochelap V A, Mel'nikov L Yu and Sokolov V N 1982 *Sov. Phys. Semicond.* **16** 746  
Kochelap V A and Sokolov V N 1988 *Phys. Status Solidi b* **146** 311
- [14] Bohnert K, Kalt H and Klingshirn C 1983 *Appl. Phys. Lett.* **43** 1088
- [15] Rossmann H, Henneberger F and Voist J 1983 *Phys. Status Solidi b* **115** K63  
Henneberger F and Rossmann H 1984 *Phys. Status Solidi b* **121** 685
- [16] Schmidt H E, Haug H and Koch S W 1984 *Appl. Phys. Lett.* **44** 787
- [17] Koch S W, Schmidt H E and Haug H 1984 *Appl. Phys. Lett.* **45** 932  
Lindberg M, Koch S W and Haug H 1986 *Phys. Rev. A* **33** 407
- [18] Gibbs H M *et al* 1985 *Phys. Rev. A* **33** 692